

Effects of High Frequency AC Currents on Cold Temperature Battery Performance

A. Hande

Member, IEEE

Electrical and Computer Engineering Department
Lake Superior State University, Sault Ste. Marie, MI 49783
Phone: (906) 635-2598, Fax: (906) 635-6663
Email: ahande@lssu.edu

T.A. Stuart

Senior Member, IEEE

Electrical Engineering Department
The University of Toledo, Toledo, OH 43606
Phone: (419) 530-8289, Fax: (419) 530-8146
Email: tstuart@uoft02.utoledo.edu

Abstract - A unique method has been developed for internally heating hybrid electric vehicle batteries at cold temperatures using high frequency alternating currents (AC). The poor performance of these batteries in cold climates is of major concern because they suffer a huge loss in capacity. Another symptom of this low performance is a dramatic increase in the series resistance of the battery, R_B , as the temperature drops. A high frequency inverter was designed to test the feasibility of AC heating. The inverter was designed for a maximum pack voltage of 200V and minimum operating frequency of 6.67 kHz while operating in the continuous conduction mode. It uses a pair of insulated gate bipolar transistors connected in a half bridge configuration. Tests were conducted on a pack of sixteen series connected nickel metal hydride batteries. Experimental results have shown that at both -20 and -30°C, 10-20 kHz AC currents at amplitudes of 60-80 A_{RMS} warmed the pack to about 25°C within a few minutes, and thereby improved the pack discharge capability.

Index Terms - Hybrid electric vehicle, Alternating current, Nickel metal hydride, High frequency inverter.

I. INTRODUCTION

Hybrid electric vehicles (HEVs) make use of alternate energy sources such as electrochemical secondary batteries, flywheels, and ultracapacitors for propulsion. However, at present virtually all of these vehicles use large packs of batteries connected in series. These batteries are perishable products and deteriorate as a result of the chemical action that proceeds during usage and storage. The cell design, temperature, and length of usage/storage are a few factors that affect the life or charge retention of these batteries [1]. Some of the more popular versions used in today's HEVs, include lead acid, nickel metal hydride (NiMH), and lithium-ion.

Every battery has a rated capacity which indicates the maximum charge that can be put into it. This is known as the full charge capacity. The actual capacity of a battery indicates the actual charge it possesses. Both these capacities are usually defined in ampere-hours (instead of coulombs) and can be calculated from the following equation:

$$\text{Battery capacity (Q)} = \int i dt \quad (1)$$

Therefore, battery capacity indicates the amount of charge it is capable of storing and delivering to an electrical load. This also depends on the rate of discharge, and the higher the rate of discharge, the lower the usable battery capacity. The actual capacity is sometimes referred to, on a percentage basis, as the state of charge (SOC). It is represented as,

$$\text{SOC} = (\text{Actual Q} / \text{Rated Q}) \times 100 \% \quad (2)$$

It is well known that Q also decreases with a decrease in ambient temperature. The degree of the ambient temperature effect on the capacity depends upon the type and quality of the electrolyte and the SOC. This decrease in battery capacity at low temperatures occurs because the viscosity of the electrolyte increases, and in some cases the electrolyte can actually freeze. This limits the flow of current from one electrode to the other, and the battery resistance increases. At very low temperatures this effect can be dramatic, and the electrolyte needs to be warmed so that the vehicle will operate satisfactorily.

At cold temperatures such as those below 0°C, battery charge and discharge become increasingly difficult. Fig.1 shows a simplified model that can be used to explain the problem for most types of batteries. The model consists of three parts:

1. An ideal voltage source, V_0 , that represents the charge storage mechanism.
2. A conventional coulomb resistance, R_c , that represents the ohmic voltage drop.
3. An equivalent resistance, R_{ov} , called the overvoltage resistance.

R_{ov} is not a resistance in the usual sense, but a component used to account for the extra energy that must be supplied to get charge into or out of V_0 [2,3]. As the battery temperature drops, R_{ov} increases because more energy is required to either charge or discharge the battery. R_{ov} is highly nonlinear with respect to the SOC and the magnitude and direction of the current, I_B . At a sufficiently low temperature and SOC, R_{ov} becomes so large that the battery is virtually unusable.

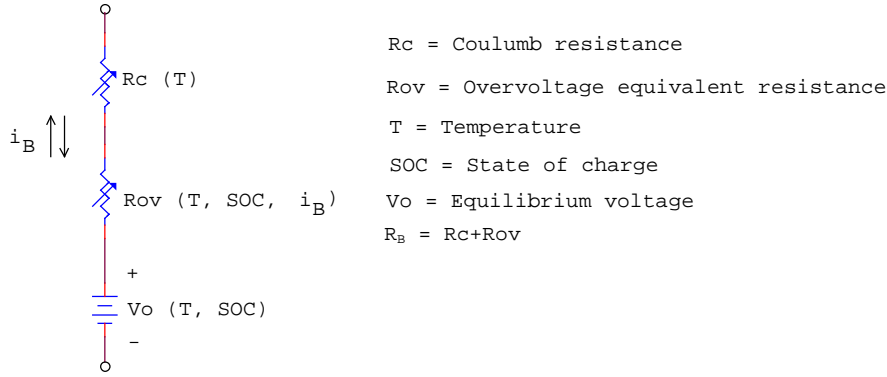


Fig.1. Battery model

Assuming V_o remains fairly constant, the detrimental effect of a large R_{ov} on discharge is obvious once R_{ov} begins to approach or exceed the load resistance. Also, a high R_{ov} seriously limits the charging ability of the battery. Because of the energy level required to force a higher current through a high R_{ov} , this also creates excessive gassing. This leads to a loss of electrolyte, and for sealed batteries the internal pressure can exceed the capacity of the relief valves. When this happens, it is quite easy to rupture the battery case.

Preliminary research has shown that external heating methods require a significant amount of time for warming the batteries since the external heat energy must penetrate the large mass of the pack [4,5]. Alternatively, it is possible to internally heat cold batteries via internal I^2R losses by circulating high frequency alternating currents (AC). This method has shown that it is possible to heat cold batteries much more rapidly as compared to external heating mechanisms and has been found to be more energy efficient as well [7-9].

Initially, 60 Hz AC heating was tested on several lead acid batteries to verify the feasibility of AC heating [6,7]. However, battery experts have indicated that each 8.33×10^{-3} sec. (60 Hz) half cycle is enough time for significant ionization to occur. This indicates that 60 Hz AC could decrease battery lifetime. However, at frequencies above 5 kHz, there is no documented evidence that a half cycle of no more than 100×10^{-6} seconds would be detrimental. A high frequency 10-20 kHz inverter was therefore designed for circulating the AC currents, and tests were conducted on a 128 V_{DC} pack comprising of sixteen series connected 8 V_{DC} 6.5 ampere hour (Ah) Panasonic NiMH batteries at cold temperatures. The inverter design details and experimental results are presented in the next few sections.

II. THE 10-20 KHZ INVERTER

Fig.2 shows the 10-20 kHz inverter circuit described in [10] with the pack divided into two halves whose voltages are V_{B1} and V_{B2} . The circuit includes a pair of insulated gate

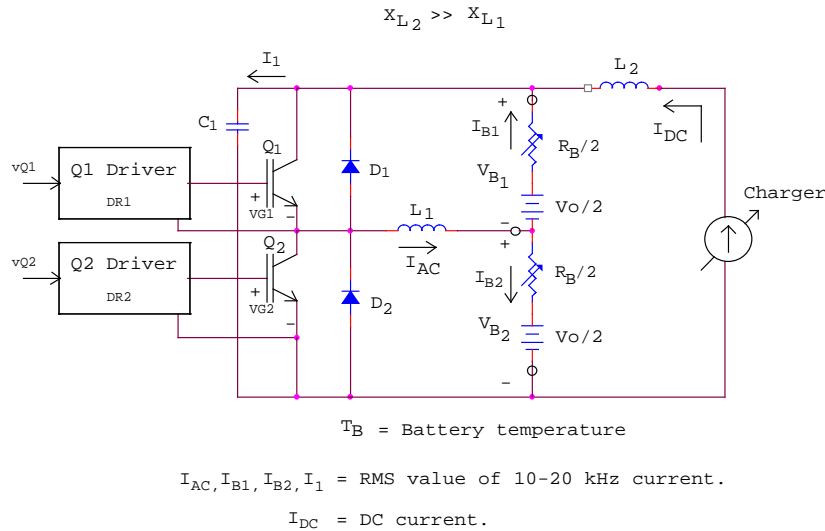


Fig.2. Battery charger with 10-20 kHz AC heater

bipolar transistors (IGBTs) Q_1 and Q_2 connected in a half bridge configuration. Anti-parallel diodes D_1 and D_2 are connected in parallel with Q_1 and Q_2 respectively. The circuit uses the variable frequency modulation technique over a frequency range that minimizes the inductor weight and size without creating excessive losses in the inductor core, coil, or the power semiconductor switches. The purpose of this circuit is to circulate an AC current between the two halves of the pack. Therefore, each half is alternately charged and discharged, and thus heated by internal $I^2R_B/2$ losses.

In Fig.2, a third connection is made to the center of the battery pack. Referring to the i_{AC} waveform in Fig.3, the V_{G1} output from the Q_1 driver card (DR_1) turns transistor Q_1 ON at t_0 . Since the voltage drops across $R_B/2$ and Q_1 are very small, the voltage from the top half of the pack, V_{B1} , is impressed across inductor L_1 . Therefore i_{AC} starts increasing linearly with time, storing energy within inductor L_1 . At t_1 , DR_1 drives V_{G1} signal to the low state. Transistor Q_1 then begins to turn OFF at t_1 and i_{AC} starts commutating through diode D_2 . i_{AC} then flows in the D_2, L_1, V_{B2} loop until it reaches zero at t_2 . In other words, the current which flows through inductor L_1 begins to conduct through the lower half of the battery pack. Thus for $0 \leq t \leq t_1$, energy is removed from V_{B1} and stored in L_1 . For $t_1 \leq t \leq t_2$, the energy in L_1 is transferred to V_{B2} .

At a time slightly before t_2 , the Q_2 driver card (DR_2) drives V_{G2} high, turning transistor Q_2 ON. It can be observed that Q_2 turns ON while current flows through the anti-parallel diode D_2 resulting in virtually zero turn-on losses in Q_2 . The turn-on losses for an IGBT are directly proportional to the square of the voltage from the collector to emitter. For a 128 V_{DC} battery pack, the voltage from collector to emitter would be approximately 64 V_{DC} for this circuit. However, by turning the IGBT ON while current is flowing through the anti-parallel diode, the collector to emitter voltage at turn-on is approximately one diode drop. The diode drop for D_2 is approximately 1 V_{DC} . Therefore, in this case the turn-on losses of Q_2 are decreased by a factor of more than 4000.

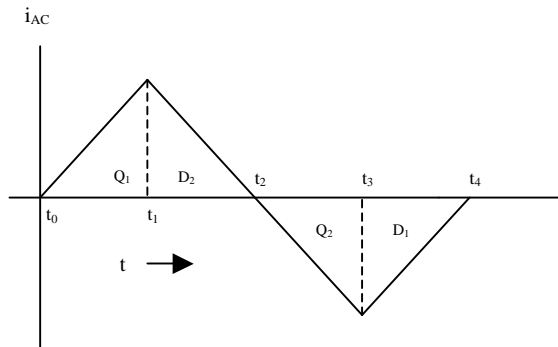


Fig.3. i_{AC} waveform for the circuit in Fig.2

Current in the anti-parallel diode D_2 continues to decrease until it reaches zero, at which time i_{AC} begins to flow into the collector of Q_2 and up through the lower half of the battery pack. As current flows through L_1 , energy is transferred from the lower half of the pack into L_1 until Q_2 turns OFF. At time t_3 , DR_2 drives V_{G2} low to turn Q_2 OFF. As Q_2 turns OFF, the current flowing through the inductor begins to flow up through the anti-parallel diode D_1 and down through the top half of the pack, i.e., the D_1, V_{B1}, L_1 loop. The voltage from the batteries is impressed across L_1 causing current i_{AC} to decrease linearly. During this period energy is transferred from L_1 into the top half of the pack. At some time prior to i_{AC} reaching zero, Q_1 is turned ON, thereby attaining virtually lossless turn-on in a manner similar to Q_2 . When i_{AC} becomes zero, diode D_1 becomes back-biased and i_{AC} once again flows through the Q_1, L_1, V_{B1} loop.

Therefore, energy is cycled between the two halves of the pack. L_2 is chosen so that $X_{L2} \gg X_{L1}$. This insures that I_{DC} remains essentially constant, and virtually no 10-20 kHz current flows through the charger. C_1 is used in Fig.2 to prevent excessive voltage transients across Q_1 and Q_2 when they turn OFF. While C_1 must be large enough to provide protection, it also should be as small as possible to minimize I_1 . This is because I_1 represents current that is siphoned away from I_{B1} and I_{B2} . To avoid overheating, a polypropylene capacitor was used for C_1 . $C_1 = 20 \mu F$ was found to provide adequate switch protection during turn OFF. The present C_1 value resulted in $I_{B1} = I_{B2} \cong 0.5 I_{AC}$. Therefore, the AC conduction losses in the pack are

$$2 \left(\frac{I_{AC}}{2} \right)^2 \cdot \frac{R_B}{2} = \frac{I_{AC}^2 R_B}{4} \quad (3)$$

Therefore, in order to achieve an effective 100 A_{RMS} heating current, $I_{AC} \cong 200 A_{RMS}$. The inverter design was first simulated using OrCAD PSpice. During the simulations, different inductance values for L_1 were used to obtain adequate I_{B1} and I_{B2} values for pack heating [11].

III. ESTABLISHING 10-20 kHz AC HEATING PARAMETERS

Preliminary 60 Hz AC heating experiments indicated that an amplitude of about 60 A_{RMS} was sufficient to revive defunct lead acid batteries at cold temperatures [6,7]. Therefore, all of the initial 10-20 kHz tests were conducted at $I_{B1} = I_{B2} = 60 A_{RMS}$.

Before starting the 10-20 kHz testing on the sixteen module NiMH pack, it was necessary to determine the appropriate AC current amplitude and time duration for a certain ambient temperature and SOC, and the power dissipated by the battery during AC heating. This is necessary for determining the proper value of I_{DC} in Fig.2, which must replace the energy used to operate the heating circuit.

Without I_{DC} , the battery will experience significant discharge. Therefore, the charger in Fig.2 must supply the losses in both the battery (P_{bat}) and the AC heating circuit (P_{heater}) to prevent significant battery discharge. Since the charger in Fig.2 will operate in the voltage regulation mode, V_0 will remain constant, but I_{DC} will vary while the heater is operating. However, I_{DC} must be limited to some upper value in order to protect the system.

Table 1 shows P_{bat} vs. time for a test conducted on a single Panasonic NiMH battery module where 60 A_{RMS} 60 Hz AC was applied for 6 minutes at -20°C and SOC = 100%. Tests were conducted at -20°C because discussions with EV/HEV experts indicated that NiMH batteries tend to lose about 90% of their capacity at this temperature. All power measurements were taken with a true RMS wattmeter at the 60 Hz source. The power loss (P_{loss}) in the test circuit was measured and found to be 122.5 W. This value was subtracted from the total loss to obtain P_{bat} for the single battery module. This value was then multiplied by sixteen to obtain P_{total} for the entire pack. Therefore, required $I_{DC} = P_{total} / \text{pack voltage}$, where pack voltage $\cong 130 V_{DC}$.

The parameters for this test were chosen to match those to be used in the subsequent 10-20 kHz test, i.e., 60 A_{RMS} at -20°C and SOC = 100%. These rather lenient initial conditions were chosen to verify the operation of the 10-20 kHz heater while the battery was at -20°C since the heater had only been operated previously with the battery at room temperature. The strategy was to verify the feasibility for this case and then proceed to more severe conditions. These results indicated a P_{bat} loss of 31.7 Watts (W) at time = 0 which decreased to 12.4 W after 6 minutes. This indicates pack losses of 507.2 W and 198.1 W respectively.

After verifying that the heater was able to sustain $I_{B1} = I_{B2} = 60 A_{RMS}$ for reasonable amount of time without any I_{DC} , it was decided to test the battery pack with the high frequency heater using the calculated values for I_{DC} in Table 1. This test was conducted at -20°C (soak time > 7 hours) with a pack SOC $\cong 55\%$. Test results shown in Table 2 indicate that the

Table 1. P_{bat} vs. time at 60 A_{RMS} / 60 Hz, SOC \cong 100%

Time (min)	Pac (W)	Pbat (W)	Ptotal (W)	Required I_{DC} (A _{DC})
0	154.2	31.7	507.2	3.90
1	146.6	24.1	385.6	2.97
2	145.0	22.5	360.0	2.77
3	137.0	14.5	232.0	1.78
4	135.9	13.4	213.9	1.65
5	135.1	12.6	202.1	1.55
6	134.9	12.4	198.1	1.52

Table 2. I_{DC} test result #1 at -20°C, SOC = 55%, $I_{B1} = I_{B2} = 60 A_{RMS}$

60 Arms		I_{DC} (A _{DC})	Total Pack V before pulse (V _{DC})
Pack DeltaV (V _{DC})	R_B (ohm)		
24.2	0.97	3	128.5
14.7	0.59	2	119.6
8.2	0.33	2	117.4
12.8	0.51	3	113
21.2	0.85	4	107.9

pack resistance, R_B , decreased by 67 % after 6 minutes, but then started to increase. This occurred due to a low value of I_{DC} , which apparently was not adequate to compensate for the losses, i.e., the pack was discharging. This is also borne out by the steady decrease in the pack voltage which is also shown in Table 2.

However, in spite of the evidence of discharge, the R_B values indicated very effective heating within 6 minutes. In an HEV, the generator current (I_{DC}) would need to be controlled to maintain a constant battery voltage while the heater is in use.

Although the required value of I_{DC} was estimated previously, these values were only based on the I^2R_B losses in the pack. It was quite evident from the above test that these I_{DC} values were too low, and it is also necessary to compensate for the heater circuit losses. If this is not done the SOC will begin to decrease when the high frequency heater is used. In order to measure losses in the heater, the pack was replaced by four large electrolytic capacitors shown in Fig.4. The capacitors were used to provide a split voltage source with low losses, but the charger must provide the entire current needed to compensate for the heating circuit loss. If

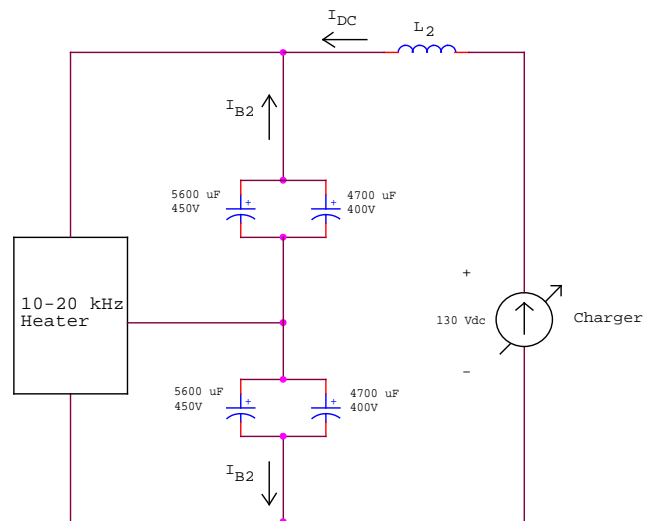


Fig.4. Measurement of heater circuit losses

the pack was used for this test, the heating circuit loss would be compensated by current from the pack plus current from the charger, and this would not provide the required value of I_{DC} .

It was found that an I_{DC} equal to about $6.6 A_{DC}$ was needed to circulate $I_{B1} = I_{B2} = 60 A_{RMS}$ at 10 kHz through the capacitor bank at $130 V_{DC}$.

$$\therefore \text{Total power needed from charger} = 130 \times 6.6 = 858 \text{ W.}$$

The equivalent series resistance (ESR) of each capacitor $\cong 20$ milliohm.

- \therefore Total ESR of capacitor bank $\cong 20$ milliohm.
- $\therefore P_{loss}$ in capacitor bank $\cong 60^2 \times 20 \times 10^{-3} = 72 \text{ W}$.
- $\therefore P_{heater} \cong 858 - 72 = 786 \text{ W}$.
- $\therefore P_{CHARGER} \cong P_{total} + P_{heater}$.
- \therefore Required $I_{DC} = P_{CHARGER} / 130$.

P_{bat} was calculated at a SOC $\cong 55\%$ in a similar manner to the method used previously, and the new values of required I_{DC} are shown in Table 3. Table 3 indicates that a total of at least 10-11 A_{DC} is required for I_{DC} at the start to sustain the pack voltage and prevent the pack from discharging.

With $I_{DC} = 10-11 A_{DC}$, tests indicated in Table 4 showed that R_B decreased by almost 74% after 6 minutes and appeared to have stabilized after 7 minutes. However, the pack voltage continued to drop from $124.68 V_{DC}$ at 0 minutes to $118.24 V_{DC}$ at the end of 6 minutes indicating that I_{DC} was still inadequate.

In order to counter the pack discharge problem during 10-20 kHz heating, the charger in Fig.2 was operated in the voltage regulation mode with the voltage set to approximately $126 V_{DC}$. This voltage corresponds to the open circuit voltage of the pack at an SOC $\cong 55\%$. This voltage was then decreased very slightly so that $I_{DC} = 0$ while the heater was off. Therefore when the heater is on, none of I_{DC} is used for increasing the SOC, but the system will draw just enough I_{DC} to compensate for the heating circuit loss and the I^2R_B loss.

Table 3. P_{bat} vs. time at $60 A_{RMS} / 60 \text{ Hz}$, SOC $\cong 55\%$

Time (min)	Pac (W)	Pbat (W)	Ptotal (W)	PCHARGER (W)	Required I_{DC} (A)
0	160.6	38.1	609.6	1395.6	10.73
1	150.5	28.0	448.5	1234.5	9.49
2	148.2	25.7	411.8	1197.8	9.21
3	142.1	19.6	313.0	1099.0	8.45
4	143.3	20.8	332.8	1118.8	8.61
5	143.7	21.2	339.2	1125.2	8.66
6	144.3	21.8	348.3	1134.3	8.72

Table 4. I_{DC} test result #2 at -20°C , SOC = 55%, $I_{B1} = I_{B2} = 60 A_{RMS}$

Time (min)	60 Arms		I_{DC} (A)	Total Pack V before pulse (V)
	Pack DeltaV (V)	R_B (ohm)		
0	27.56	1.10	11	124.68
3	12.80	0.51	10	119.28
6	7.28	0.29	10	118.24
7	6.92	0.27	10	119.08

Test results in Table 5 indicate that about $20 A_{DC}$ I_{DC} was required at the start of the test and it decreased to $17 A_{DC}$ after 8 minutes which is considerably higher than the estimated value from previous tests. R_B again decreased by almost 73% after 6 minutes. However, this time the pack voltage remained constant at approximately $126 V_{DC}$ throughout the test. Thus, an I_{DC} limit of about $20 A_{DC}$ is required to account for the heating circuit losses and the I^2R_B losses at the start of the heating cycle.

IV. ESTIMATING INTERNAL BATTERY TEMPERATURE BY MEASURING R_B

While I_{AC} is applied, it is very important that the internal temperature of the battery, T_{bat} , be known in order to prevent overheating and possible damage. Although it is possible to measure the battery case temperature using thermocouples or thermistors, this does not provide a method to obtain a correct estimation of T_{bat} . However, T_{bat} can be estimated by measuring the battery series resistance, R_B . Therefore, the figure of merit used for the 10-20 kHz tests was the pack series resistance, R_B . R_B was measured using an AeroVironment ABC150 power processing system [12].

Measurements were made with the aid of its remote operating software (ROS) [13] using a personal computer. The data acquisition was carried out using a National Instruments PCI-6024E NI-DAQ card [14] that interfaced with a sixteen channel Analog Devices 5B Series signal conditioning module [15]. Eight channels were used for measuring eight pairs of battery voltages and the remaining eight were used to sense the module temperatures as described in [11].

Table 5. I_{DC} test result #3 at -20°C , SOC = 55%, $I_{B1} = I_{B2} = 60 A_{RMS}$

Time (min)	60 Arms		I_{DC} (A)	Total Pack V before pulse (V)
	Pack DeltaV (V)	R_B (ohm)		
0	24.32	0.97	20	125.64
3	10.92	0.44	18	125.72
6	6.64	0.26	18	125.88
8	5.44	0.22	17	125.56

A pulse current profile (PCP) pulse waveform, I_0 , having amplitudes of $25 A_{DC} / 2$ seconds on both the discharge and charge cycles was applied as shown in Fig.5. Fig.6 shows the pulse test set-up. If ΔV_0 = the V_0 voltage drop (during the discharge cycle) when the (+) I_0 pulse is applied,

$$R_B = \Delta V_0 / I_0 \tag{4}$$

The (-) pulse was used to replace the charge taken by the (+) pulse. R_B was measured after the batteries were soaked in a temperature chamber for several hours at various temperatures from $25^\circ C$ to $-30^\circ C$. After a sufficiently long soak, T_{bat} can be assumed to be equal to its external ambient temperature, and therefore can be plotted vs. R_B . These tests were repeated at various SOC values. With this data, R_B can be used to determine the internal temperature during the subsequent AC heating tests.

Tests were first carried out on a single 6.5 Ah Panasonic NiMH battery in order to see the effects of SOC and T_{bat} on R_B . R_B was calculated using equation 4 at various temperatures and SOC's, and the results are shown in Table 6.

As expected, R_B increased with a decrease of temperature. However, it is almost constant for temperatures of $25^\circ C$ and above and therefore R_B cannot be used to identify battery temperatures above $25^\circ C$. Also, this test revealed that R_B is very insensitive to the SOC. Since sixteen battery modules

were used in the pack, the values of R_B in Table 6 were multiplied by sixteen and the resulting R_B was plotted vs. T_{bat} in Fig.7. This plot was then used to predict T_{bat} from R_B measurements in subsequent tests.

V. 10-20 kHz AC HEATING TEST RESULTS

Tests at $-20^\circ C$ and SOC = 55% showed that it is possible to heat the pack to room temperature within about 6-8 minutes by circulating a 10-20 kHz 60 A_{RMS} AC current [7-9]. However, a time lag of even 6 minutes may be unacceptable for HEV applications. Therefore the effects of higher AC amplitudes were studied. Tests at different cold temperatures and SOC's also were conducted to determine the effect of both of these variables.

To speed up the heating process, AC at amplitudes above 60 A_{RMS} were circulated through the pack. Fig.8 shows the results obtained after soaking the battery pack for 5 hours at $-20^\circ C$ with an SOC \cong 55%. Before applying the AC, $T_{bat} \cong -20^\circ C$. T_{bat} then increased to about $20^\circ C$ after 6 minutes of 60 A_{RMS} AC circulation. As expected, when the amplitude of AC was increased the heating process sped up. With 70 A_{RMS} AC circulation, about 4 minutes were needed to heat the pack to $20^\circ C$, and with 80 A_{RMS} , only about 3 minutes were needed.

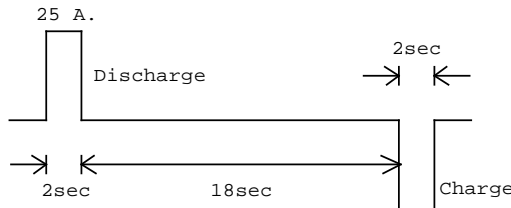


Fig.5. I_0 characterization profile

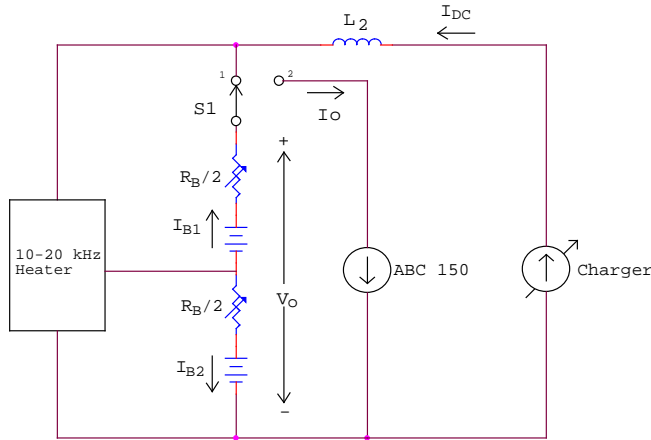


Fig.6. I_0 pulse test circuit with 10-20 kHz heating

Table 6. R_B vs. T_{bat} at different SOC's

T_{bat} (deg C.)	R_B (milliohm)			
	SOC=25%	SOC=55%	SOC=75%	SOC=100%
45	11.2	11.2	11.2	9.6
35	11.2	11.2	11.2	11.2
25	14.4	12.8	14.4	11.2
10	22.4	20.8	22.4	20.8
0	27.2	25.6	27.2	28.8
-10	41.6	38.4	43.2	43.2
-20	65.6	64.0	70.4	64.0

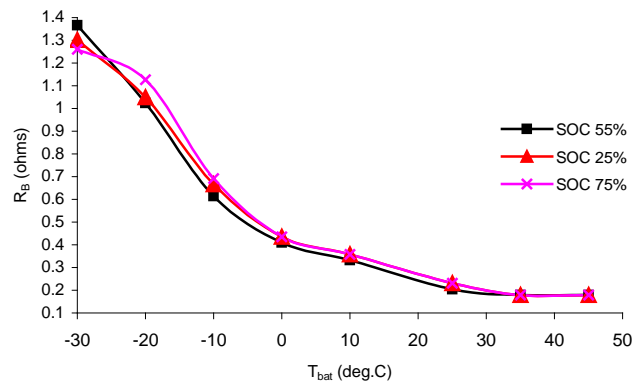


Fig.7. R_B vs. T_{bat} at different SOC's

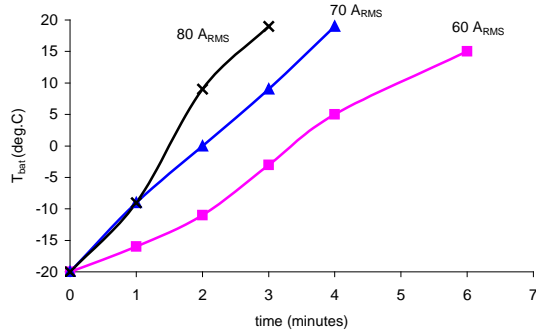


Fig.8. T_{bat} v time @ -20°C , $\text{SOC} \approx 55\%$

In order to observe the effects of AC heating at different SOC's, tests were conducted at SOC's of 25%, 55%, and 75% using AC at an amplitude of $60 A_{RMS}$. Fig.9 shows the results obtained after soaking the pack for 5 hours at -30°C and circulating $60 A_{RMS}$ with SOC's of 25%, 55%, and 75%. In this case, about 6 minutes were needed to heat the pack to 15°C when the pack SOC was 75%, and more time was needed when the SOC was lower. As shown by the plots for $\text{SOC} = 55\%$, T_{bat} was still less than 15°C after 7 minutes, and for $\text{SOC} = 25\%$ T_{bat} was just above 10°C after 8 minutes. This indicates that for colder temperatures the SOC does have some effect on the heating time.

In order to verify whether 10-20 kHz heating improved the discharge capability of the NiMH pack at cold temperatures, discharge tests were conducted using the test set-up in Fig.6. The results obtained at -20°C are shown in Fig.10. Tests were conducted at three SOC's viz. 25%, 55%, and 75%. At $\text{SOC} = 25\%$, the discharge Ah doubled from 0.45 Ah to 0.9 Ah after 6 minutes of $60 A_{RMS}$ heating. At $\text{SOC} = 55\%$, the discharge Ah improved from 1.99 Ah to 2.84 Ah, an increase of 43%. Similarly, there was an improvement of about 17% at $\text{SOC} = 75\%$. The results were more prominent at -30°C (refer Fig.11). At $\text{SOC} = 25\%$, the discharge Ah without AC equaled 0.3 Ah and improved to 0.95 Ah after 6 minutes of $60 A_{RMS}$ heating. At $\text{SOC} = 55\%$, the discharge Ah improved from 0.5 Ah to 2.59 Ah, an increase of more than 5 times. At

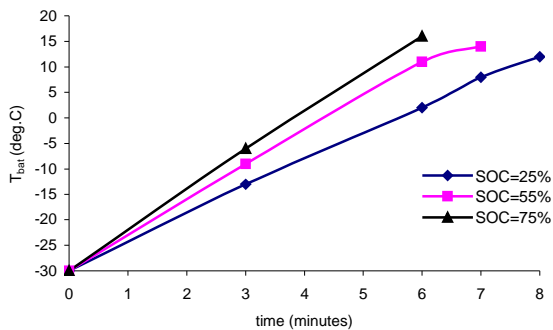


Fig.9. T_{bat} v time @ -30°C , $60 A_{RMS}$

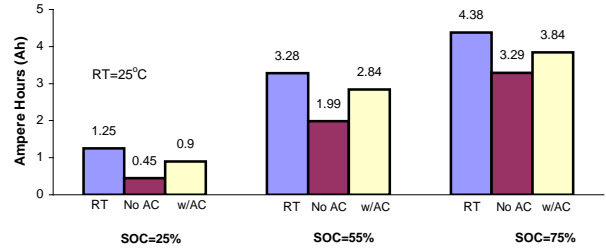


Fig.10. Discharge tests at -20°C

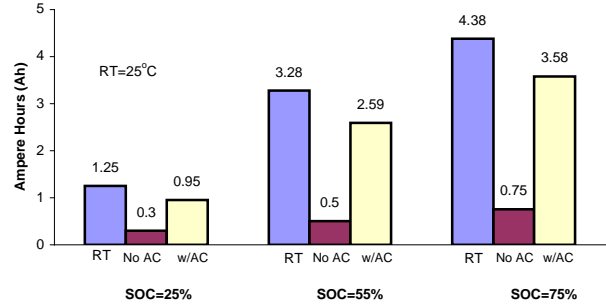


Fig.11. Discharge tests at -30°C

$\text{SOC} = 75\%$, the discharge Ah without AC equaled 0.75 Ah and it increased to 3.58 Ah after 6 minutes of AC circulation.

VI. CONCLUSIONS

A 10-20 kHz inverter was designed in order to observe the effects of high frequency AC currents on cold temperature battery performance. Tests were conducted on a pack of sixteen series connected Panasonic NiMH batteries. The test conditions were designed to simulate those on an HEV where a generator would be available to replace the energy lost in the heating process. Present practice in many HEV applications is to provide a small lead acid battery to start the internal combustion engine (ICE) and thus the generator. This is especially important for very low temperature environments where the nickel metal hydride battery would be unable to start the ICE.

These tests show that at both -20°C and -30°C , reasonable values of 10-20 kHz AC current can restore the internal battery temperature, T_{bat} , to a value fairly close to 25°C within a few minutes. However, it is also evident that it is absolutely necessary to simultaneously use a DC generator (charger) to replace the heating losses or the battery will discharge rapidly. Table 5 shows that about $19-20 A_{DC}$ I_{DC} is required to compensate for the heating circuit losses and the $I^2 R_B$ losses in the pack. A technique was developed to estimate the internal temperature of the battery, T_{bat} , during heating by measuring the battery series resistance, R_B , at known values of T_{bat} . The resulting plot of R_B vs. T_{bat} for different SOC's in Fig.7 was used to predict T_{bat} by measuring

R_B after the AC heating had been applied. Additional 60 A_{RMS} discharge tests also indicated an improvement in pack discharge capability at cold temperatures of -20 and -30°C. Further testing might be required to obtain better values for the AC amplitude and frequency for faster heating.

ACKNOWLEDGMENT

This project was supported by grants from the US Department of Energy National Renewable Energy Laboratory (NREL) and DaimlerChrysler, AG, and conducted at University of Toledo's Power Electronics Laboratory (PEL). The author would like to acknowledge the advice and assistance provided by Dr. Ahmad Pesaran (NREL).

REFERENCES

- [1] D.Linden, "Handbook of Batteries and Fuel Cells", McGraw-Hill, 1995.
- [2] D.Berndt, "Maintenance-Free Batteries", 2nd Ed., Research Studies Press Ltd., Taunton, England, 1997.
- [3] D.Rand, R.Woods, and R.Dell, "Batteries for Electric Vehicles", Research Studies Press Ltd., Taunton, England, 1998.
- [4] A.Pesaran, A.Vlahinos, and T.Stuart, "Cooling and Preheating of Batteries in Hybrid Electric Vehicles", 6th ASME-JSME Thermal Engineering Joint Conference Proceedings, Hawaii Island, Hawaii, March 16-20, 2003.
- [5] A.Vlahinos and A.Pesaran, "Energy Efficient Battery Heating in Cold Temperatures", SAE Future Car Congress Proceedings, paper number 2002-01-1975, VA, June 2002.
- [6] T.Stuart and A.Hande, "AC Battery Heating for Cold Climates", EnV 2001 Conference Proceedings, Engineering Society of Detroit, Southfield, MI, June 10-13, 2001.
- [7] A.Hande, "AC Battery Heating for Cold Climates", Ph.D. Dissertation, The University of Toledo, Toledo, OH, December 2002.
- [8] T.Stuart and A.Hande, "AC Heating for EV/HEV Batteries", 7th IEEE Workshop on Power Electronics in Transportation (WPET 2002) Conference Proceedings, pp.119-124, Detroit, MI, October 24-25, 2002.
- [9] T.Stuart and A.Hande, "HEV Battery Heating using AC Currents", Journal of Power Sources, Vol.129, Issue.2, pp.368-378, April 2004.
- [10] C.Ashtiani and T.Stuart, "Circulating Current Battery Heater", U. S. Patent 6,259,229, July 10, 2001.
- [11] A.Hande, "A High Frequency Inverter for Cold Temperature Battery Heating", 9th IEEE Workshop on Computers in Power Electronics (COMPEL 2004) Conference Proceedings, University of Illinois, Urbana-Champaign, IL, August 15-18 2004.
- [12] "ABC-150 Remote Operating System Manual", Revision 1.0, AeroVironment Inc., 1998.
- [13] "ABC-150 Power Processing System", AeroVironment Inc., 2000 <http://www.aerovironment.com/area-pps/prod-serv/abc-150.html>.
- [14] "Low-Cost E Series Multifunction DAQ 12 or 16-Bit, 200 kS/s, 16 Analog Inputs", National Instruments Corporation, 2004, http://www.ni.com/pdf/products/us/4daqsc202-204_ETC_212-213.pdf.
- [15] "5B Series Overview", Analog Devices, 2004, http://www.analog.com/Analog_Root/static/marketSolutions/ios/catalog/5b/5b_intro.html.